

Biogeosciences Discussions is the access reviewed discussion forum of *Biogeosciences*

CO₂ backflux matters

A. Oschlies

Impact of atmospheric and terrestrial CO₂ feedbacks on fertilization-induced marine carbon uptake

A. Oschlies

IFM-GEOMAR, Leibniz-Institut für Meereswissenschaften, Kiel, Düsternbrooker Weg 20,
24105 Kiel, Germany

Received: 2 April 2009 – Accepted: 9 April 2009 – Published: 23 April 2009

Correspondence to: A. Oschlies (aoschlies@ifm-geomar.de)

Published by Copernicus Publications on behalf of the European Geosciences Union.

Title Page

Abstract

Introduction

Conclusions

References

Tables

Figures



Back

Close

Full Screen / Esc

Printer-friendly Version

Interactive Discussion



Abstract

The sensitivity of oceanic CO₂ uptake to alterations in the marine biological carbon pump, such as brought about by natural or purposeful ocean fertilization, has repeatedly been investigated by studies employing numerical biogeochemical ocean models.

It is shown here that the results of such ocean-centered studies are very sensitive to the assumption made about the response of the carbon reservoirs on the atmospheric side of the sea surface. Assumptions made include prescribed atmospheric *p*CO₂, an interactive atmospheric CO₂ pool exchanging carbon with the ocean but not with the terrestrial biosphere, and an interactive atmosphere that exchanges carbon with both oceanic and terrestrial carbon pools. The impact of these assumptions on simulated annual to millennial oceanic carbon uptake is investigated for a hypothetical increase in the C:N ratio of the biological pump and for an idealized enhancement of phytoplankton growth. Compared to simulations with interactive atmosphere, using prescribed atmospheric *p*CO₂ overestimates the sensitivity of the oceanic CO₂ uptake to changes in the biological pump, by about 2%, 25%, 100%, and >500% on annual, decadal, centennial, and millennial timescales, respectively. Adding an interactive terrestrial carbon pool to the atmosphere-ocean model system has a small effect on annual timescales, but increases the simulated fertilization-induced oceanic carbon uptake by about 4%, 50%, and 100% on decadal, centennial, and millennial timescales, respectively. On longer than decadal timescales, a substantial fraction of oceanic carbon uptake induced by natural or purposeful ocean fertilization may not come from the atmosphere but from the terrestrial biosphere.

1 Introduction

The oceanic control on atmospheric CO₂ is the result of a complex interplay of physical, chemical, and biological processes. It primarily arises from the temperature-dependent solubility of CO₂ (solubility pump) and the photosynthetic conversion of dissolved inor-

BGD

6, 4493–4525, 2009

CO₂ backflux matters

A. Oschlies

Title Page

Abstract

Introduction

Conclusions

References

Tables

Figures



Back

Close

Full Screen / Esc

Printer-friendly Version

Interactive Discussion



CO₂ backflux matters

A. Oschlies

[Title Page](#)[Abstract](#)[Introduction](#)[Conclusions](#)[References](#)[Tables](#)[Figures](#)[Back](#)[Close](#)[Full Screen / Esc](#)[Printer-friendly Version](#)[Interactive Discussion](#)

ganic carbon into carbon-containing organic particles that may sink away from immediate contact with the atmosphere (biological pump) (Volk and Hoffert, 1985). While the ongoing global warming is often assumed to affect mainly the solubility pump with relatively minor impacts on the biological pump (Sarmiento and Le Quéré, 1996), there is more and more evidence for possibly significant disturbances of the marine biological pump: Increasing levels of sea-water CO₂ are expected to impact on the marine biology, e.g., by making it harder to form calcium carbonate shells (Riebesell et al., 2000) or by affecting the ratio of the biotic carbon-to-nutrient drawdown (Riebesell et al., 2007). At the same time, the surface ocean is fertilized by a rapidly increasing atmospheric input of nitrogen to the oceans due to emissions from the combustion of fossil fuels as well as from the production and use of fertilizers (Duce et al., 2008). Purposeful ocean fertilization, in particular using iron, is also discussed as a possible way to reduce the acceleration of atmospheric CO₂ concentrations in response to anthropogenic emissions (Lampitt et al., 2008).

A number of modeling studies have addressed the potential impact of such disturbances of the biological pump on the oceanic carbon uptake. For example, Schneider et al. (2004) investigated the impact of CO₂-dependent C:N ratios of particulate organic matter formation and export. They found that by increasing the molar C:N ratio from 7.1 in year 1770 to 8.1 in year 2000 and thereafter, the oceanic carbon uptake increased by 70 PgC by AD 2100 compared to a simulation with a constant C:N ratio of 7.1. A recent study by Oschlies et al. (2008) assumed a somewhat larger CO₂-dependent increase in C:N ratios from 6.7 in AD 1765 to 8.4 in AD 2100 which, in their model, resulted in a *smaller* additional oceanic CO₂ uptake of 34 PgC by AD 2100. At first sight, there seems to be significant (~factor 2) ambiguity in the simulated impact of very similar changes in the marine biology on the oceanic carbon uptake.

Similarly different results have been reported for model studies investigating the impact of atmospheric dust supply and the associated fertilization with the micronutrient iron: Forcing a model with different dust scenarios including switches from interglacial to glacial conditions, Moore et al. (2006) reported that, on decadal timescales, 45%

to 60% of a dust-related increase in carbon export by the marine biological pump was exporting carbon removed from the atmospheric CO₂ pool via air-sea exchange. On switching from present-day to last-glacial maximum dust fields, Bopp et al. (2003), on the other hand, found that merely 25% of the additional carbon exported by the biological pump was derived from the atmosphere on decadal timescales.

The third example refers to simulated purposeful iron fertilization: For simulated localized iron fertilization in the tropical Pacific, Gnanadesikan et al. (2003) found that only about 10% of the initial pulse of carbon exported out of the surface layer were actually removed from the atmosphere on a 10- to 100-year timescale. A similar study by Jin et al. (2008) reported, on the contrary, that more than 75% of the carbon exported in response to localized iron fertilization in the equatorial Pacific came from the atmosphere, though this percentage was reduced to 34% when the entire Pacific was fertilized.

In all above examples, the simulated ratio of changes in air-sea CO₂ flux to changes in biotic carbon export, which has been referred to as atmospheric uptake efficiency (Jin et al., 2008), differs by a factor of about 2 or more among different published model results. This difference is larger than the 19% scatter in simulated anthropogenic carbon uptake for a range of different circulation models participating in the Ocean Carbon Model Intercomparison Project (OCMIP) (Orr et al., 2001). However, while the OCMIP simulations followed a common protocol for the treatment of the biological pump and air-sea gas exchange, this was not the case for the above-mentioned studies looking at sensitivities of air-sea CO₂ flux to changes in the biological pump.

Jin et al. (2008) showed that part of the discrepancy among the different studies could be attributed to the different depth distribution of fertilization within the euphotic zone. The closer to the sea surface the biology is altered, the higher is the likelihood that changes in export production are felt by the atmosphere. This is of particular relevance in tropical regions with shallow mixed layers and deep chlorophyll maxima where biotically induced air-sea CO₂ flux shows little correlation with local export production (Oschlies and Kähler, 2004). The Jin et al. (2008) argument applies specifically to dif-

CO₂ backflux matters

A. Oschlies

[Title Page](#)[Abstract](#)[Introduction](#)[Conclusions](#)[References](#)[Tables](#)[Figures](#)[Back](#)[Close](#)[Full Screen / Esc](#)[Printer-friendly Version](#)[Interactive Discussion](#)

ferences between early models simulating iron fertilization by restoring euphotic zone nutrient levels to zero and more detailed marine ecosystem models that resolve biological processes within the euphotic zone. It is probably of less relevance to explain differences between the relatively similar ecosystem models used by Bopp et al. (2003) and Moore et al. (2006) or the varying C:N ratios employed by Schneider et al. (2004) and Oschlies et al. (2008).

Here a different hypothesis will be investigated, namely that differences in the treatment of the atmospheric boundary condition can explain part of the differences among the different model studies. It appears that all those simulations that revealed high ratios of anomalous air-sea CO₂ fluxes to anomalous biotic carbon-export fluxes used prescribed atmospheric CO₂ levels (Schneider et al., 2004; Moore et al., 2006; Jin et al., 2008). On the other hand, all simulations that allowed atmospheric CO₂ levels to vary in response to air-sea CO₂ fluxes, yielded lower ratios of anomalous air-sea CO₂ fluxes to anomalous oceanic carbon-export fluxes (Bopp et al., 2003; Gnanadesikan et al., 2003; Oschlies et al., 2008). Earlier studies have already acknowledged a systematic overestimation of the impact of changes in the biological pump on oceanic carbon uptake by simulations using fixed atmospheric pCO₂ (e.g., Schneider et al., 2004; Jin et al., 2008; Oschlies et al., 2008). A, to the author's knowledge, first quantitative estimate of this overestimate was given by Jin et al. (2008) who referred to a paper in preparation by Sarmiento et al., according to which simulations with interactive atmospheric carbon pool resulted in a 20% reduction in fertilization-induced oceanic CO₂ uptake over 10 years (and 50% over 100 years) compared to simulations with fixed atmospheric pCO₂. The current study was performed independently and will investigate not only the feedback arising from an interactive atmosphere, but also the feedbacks arising from the exchange of carbon between the atmosphere and the terrestrial biosphere on annual to millennial timescales. As long as the timescales considered do not exceed many thousands of years, weathering feedbacks can be neglected and will not be considered in this paper. A main result is that both atmospheric and terrestrial CO₂ feedbacks can lead to significant modifications in the response of the marine carbon

[Title Page](#)[Abstract](#)[Introduction](#)[Conclusions](#)[References](#)[Tables](#)[Figures](#)[Back](#)[Close](#)[Full Screen / Esc](#)[Printer-friendly Version](#)[Interactive Discussion](#)

uptake to disturbances in the biological pump.

The paper is organized as follows: After introducing the model experiments in the following section, Sect. 3 will examine the atmospheric and terrestrial feedbacks for the example of $p\text{CO}_2$ sensitive C:N ratios. The relevance of different time and space scales considered in the perturbation of the biological pump will be investigated for idealized experiments with enhanced phytoplankton maximum growth rates in Sect. 4. A concluding section ends the paper.

2 Model

The model used in this paper is the University of Victoria (UVic) Earth System Climate Model (Weaver et al., 2001) version 2.8 essentially as described by Schmittner et al. (2008), except for the molar C:N ratio of 6.6 and the molar O_2 :N ratio of 10.6. It includes a simple marine ecosystem model and an active terrestrial vegetation and carbon cycle component, which is based on the Hadley Centre's TRIFFID model (Cox et al., 2000). The trace nutrient iron is not explicitly included. By tuning the biological parameters (in particular the relatively low phytoplankton maximum growth rate of 0.13 day^{-1} at 0°C), the model nevertheless achieves a reasonable fit to observed marine biogeochemical tracer distributions (Schmittner et al., 2005, 2008).

2.1 Model experiments

Two different scenarios of disturbances of the marine biological pump are discussed in the following sections: The impact of $p\text{CO}_2$ -sensitive C:N ratios (Sect. 3) and the impact of enhanced phytoplankton maximum growth rates, which may be viewed as idealized ocean fertilization scenario (Sect. 4). All model runs start from the same model state that was obtained by spinning up the model for 7000 years under under pre-industrial prescribed atmospheric $p\text{CO}_2$ of $280 \mu\text{atm}$ and with a molar C:N ratio of 6.6. For each scenario, four different model configurations were employed (Fig. 1),

Title Page

Abstract

Introduction

Conclusions

References

Tables

Figures

◀

▶

◀

▶

Back

Close

Full Screen / Esc

Printer-friendly Version

Interactive Discussion



differing only in the treatment of the atmospheric and terrestrial carbon pools and their interaction with each other:

- **ATCO₂const**: Atmospheric $p\text{CO}_2$ is fixed at $280 \mu\text{atm}$. In consequence, annual mean climate and terrestrial carbon stocks stay constant. This configuration essentially assumes an infinitely large atmospheric carbon pool such that CO_2 concentrations do not change in response to CO_2 exchange with the ocean. Total carbon is not conserved.
- **VEGconst**: Uses a finite atmospheric carbon reservoir (initially 573 PgC, corresponding to $280 \mu\text{atm}$), which can exchange carbon with the ocean (initially 37 300 PgC) such that total carbon is conserved. No exchange is allowed with the terrestrial carbon pool.
- **COUPLED**: Uses the same initial carbon reservoir sizes as experiment VEGconst, but allows the atmosphere to exchange carbon with both the ocean and the terrestrial carbon pool (initially 1350 PgC in soils and 600 PgC in vegetation), such that total carbon is conserved.
- **CLIMconst**: Uses the same initial carbon reservoir sizes as experiment COUPLED and allows both ocean and terrestrial vegetation to exchange carbon with the atmosphere, but assumes constant atmospheric $p\text{CO}_2=280 \mu\text{atm}$ in the atmosphere's radiation budget. Note that this ensures only an approximately constant climate, which can still change in response to CO_2 -induced terrestrial albedo changes. See text below.

3 Impact of $p\text{CO}_2$ sensitive C:N ratios

This section investigates the oceanic carbon uptake that may result from a possible increase in the ratio of carbon to nitrogen drawdown in response to increasing CO_2 levels in the atmosphere and in the ocean surface waters. There is some evidence from

BGD

6, 4493–4525, 2009

CO₂ backflux matters

A. Oschlies

Title Page

Abstract

Introduction

Conclusions

References

Tables

Figures

◀

▶

◀

▶

Back

Close

Full Screen / Esc

Printer-friendly Version

Interactive Discussion



CO₂ backflux matters

A. Oschlies

[Title Page](#)[Abstract](#)[Introduction](#)[Conclusions](#)[References](#)[Tables](#)[Figures](#)[◀](#)[▶](#)[◀](#)[▶](#)[Back](#)[Close](#)[Full Screen / Esc](#)[Printer-friendly Version](#)[Interactive Discussion](#)

mesocosm experiments for such an increase in C:N drawdown with $p\text{CO}_2$ (Engel et al., 2004; Riebesell et al., 2007), and model studies have investigated the hypothetical impacts of a $p\text{CO}_2$ sensitive stoichiometry on the oceanic carbon uptake (Schneider et al., 2004; Oschlies et al., 2008). The current study investigates the sensitivity of the simulated impact on the oceanic carbon uptake to carbon feedbacks on the atmospheric side of the sea surface.

Interpolating the mesocosm-derived $p\text{CO}_2$ dependence of the of C:N drawdown by the biological pump (Riebesell et al., 2007), the temporal evolution of the model's C:N ratio is assumed to follow observed and predicted atmospheric $p\text{CO}_2$. Here, historical data are used for the period 1765 until 1990, and the IS92 scenario (Houghton et al., 1997) is used for the period 1990 until 2100, by which the model's C:N ratio reaches 7.98 (Fig. 2a). With respect to the assumed pre-industrial C:N ratio of 6.6, this corresponds to an increase in molar C:N ratios by about 21%. The setup is similar to that used by Oschlies et al. (2008), except for the use of prescribed anthropogenic CO₂ emissions in that study, with C:N ratios diagnosed from the model's actual atmospheric CO₂. The current study, in contrast, does not explicitly include CO₂ emissions and “only” prescribes the evolution of C:N ratios, which is identical over all model runs irrespective of the modeled atmospheric CO₂ levels.

All four model configurations introduced in the previous section were started from the same spun up state in AD 1765 and integrated until AD 2100. The increase in simulated biotic carbon export in response to the increasing C:N ratios from about 7 PgC/yr in year 1765 to more than 8.4 PgC/yr in model year 2100 is very similar among all model runs (Fig. 2b, Table 1). Below, it will be shown that despite this close agreement in simulated export production, oceanic CO₂ uptake differs considerably among the different model runs.

3.1 Feedbacks from the atmospheric carbon pool

Most model studies investigating changes in the marine biological pump have, so far, neglected possible feedbacks from the terrestrial carbon pool. It is therefore appropri-

CO₂ backflux matters

A. Oschlies

[Title Page](#)[Abstract](#)[Introduction](#)[Conclusions](#)[References](#)[Tables](#)[Figures](#)[Back](#)[Close](#)[Full Screen / Esc](#)[Printer-friendly Version](#)[Interactive Discussion](#)

ate to first investigate the results of the two experiments ATCO₂const and VEGconst, which both keep the carbon content of the terrestrial vegetation and soils constant. Simulated atmospheric CO₂, by definition, stays constant at 280 μatm in experiment ATCO₂const and drops by 9.7 μatm by AD 2100 in run VEGconst on introducing the temporally increasing C:N ratios (Fig. 3a). The increase in the oceanic carbon inventory associated with the enhanced export of organic carbon is twice as large in run ATCO₂const compared to VEGconst (Fig. 3b: 40.6 PgC and 20.1 PgC, respectively, see also Table 1). The carbon taken up by the ocean from the atmosphere in experiment VEGconst lowers atmospheric pCO₂. This reduces the air-sea CO₂ partial pressure difference and therefore leads to a backflux of CO₂ from the surface ocean to the atmosphere. No such backflux occurs in run ATCO₂const.

The comparison of VEGconst and ATCO₂const reveals that, for the simulated case of globally uniform changes in C:N ratios, the backflux included in model VEGconst compensates about 50% of the original air-sea carbon flux induced by the perturbation of the biological pump in run ATCO₂const. In year 2100 the simulated air-sea CO₂ flux reaches 0.54 PgC/yr in run ATCO₂const and 0.27 PgC/yr in run VEGconst (Fig. 4a). It turns out that in experiment ATCO₂const 38% of the additional carbon exported in response to the elevated C:N ratios is derived from the atmosphere, whereas only 20% is derived from the atmosphere in run VEGconst (Fig. 4b). This factor 2 difference in atmospheric uptake efficiency is similar to that found among earlier studies referred to in the introduction.

3.2 Feedbacks from the terrestrial carbon pool

Once the terrestrial vegetation is allowed to exchange carbon with the atmosphere in experiment COUPLED, oceanic carbon uptake induced by enhanced C:N ratios exceeds the amount simulated by VEGconst by about 50% (Fig. 3b). The main reason for this increase is that modeled terrestrial primary production is sensitive to atmospheric CO₂ whereas respiration is not. Primary production is reduced at lower atmospheric CO₂ levels (assuming otherwise unchanged environmental conditions), which leads to

CO₂ backflux matters

A. Oschlies

[Title Page](#)[Abstract](#)[Introduction](#)[Conclusions](#)[References](#)[Tables](#)[Figures](#)[◀](#)[▶](#)[◀](#)[▶](#)[Back](#)[Close](#)[Full Screen / Esc](#)[Printer-friendly Version](#)[Interactive Discussion](#)

a net flux of carbon from the terrestrial carbon pool to the atmosphere. The UVic model has a sensitivity of land carbon storage to atmospheric $p\text{CO}_2$ of about $1.2 \text{ PgC}/\mu\text{atm}$ estimated from climate change simulations over essentially the same time interval as considered here (Friedlingstein et al., 2006). In order to reduce atmospheric $p\text{CO}_2$ by $1 \mu\text{atm}$, the ocean now has to take up not only 2.05 PgC of the atmosphere's carbon equivalent of $1 \mu\text{atm}$, but also 1.2 PgC from the terrestrial biosphere. That is, the interactive carbon pool seen by the ocean on the atmospheric side of the sea surface has increased by almost 60% in run COUPLED compared to experiment VEGconst.

Compared to the VEGconst run, atmospheric $p\text{CO}_2$ decreases less (Fig. 3a), allowing more CO_2 to invade the ocean (Fig. 3b). The negative terrestrial vegetation feedback on atmospheric CO_2 levels is thus equivalent to a positive feedback on oceanic CO_2 uptake. Note, that this feedback depends on the CO_2 fertilization effect on the terrestrial biosphere. The CO_2 sensitivity and its magnitude in the terrestrial component of the UVic Earth System model are common among current coupled carbon-climate models (Friedlingstein et al., 2006). However, the degree of realism of the modeled magnitude of this feedback is under debate (e.g., Sokolov et al., 2008).

3.3 Feedbacks from climate change

The perturbation applied to the biological pump in the above experiments consists in a prescribed change in the C:N ratio. This perturbation differs from anthropogenic greenhouse gas perturbations as it immediately affects the biological pump. Changes in the marine carbon cycle then affect atmospheric CO_2 and, in turn, cause some climate change in experiments VEGconst and COUPLED. As a result of the variations in C:N ratios considered, atmospheric CO_2 concentrations decline by less than $10 \mu\text{atm}$ and induce a global cooling of less than 0.07°C (Fig. 3d) in runs VEGconst and COUPLED, but not in CLIMconst. At the higher temperatures of CLIMconst, respiration rates are higher and the terrestrial vegetation loses about 3 PgC more carbon by year 2100 compared to run COUPLED. Of this extra carbon released into the atmosphere, only about 1 PgC stay in the atmosphere, whereas 2 PgC are taken up by the ocean. Com-

pared to the total oceanic uptake of 28.9 PgC simulated by run COUPLED, this feedback from climate change amounts to 9%. Thus, the sensitivity of the biological-pump driven oceanic carbon uptake to climate change is small compared to the sensitivities to atmospheric and terrestrial carbon feedbacks.

4 Impact of enhanced phytoplankton maximum growth rates

While the experiments of the previous section assumed a globally uniform perturbation of the biological pump on the centennial timescale of the anthropocene, this section considers the idealized scenario of an instantaneous switch in phytoplankton growth rate in order to investigate the impact of atmospheric and terrestrial carbon feedbacks on different timescales and for different regional patterns of the perturbation. The assumed perturbation is a large increase in phytoplankton maximum growth rates from 0.13 day⁻¹ in the control experiment to 10.0 day⁻¹ (at 0°C) in the perturbation experiments beginning at time zero. The enhanced growth rate is applied either globally or limited to the tropical ocean between 18° S and 18° N or to the Southern Ocean south of 30° S, which both include large HNLC (high nutrient, low chlorophyll) areas.

These experiments can be viewed as (yet another) indirect attempt to estimate the potential impact of large-scale iron fertilization on the global carbon cycle. The enhanced growth-rate approach taken here is intermediate between more idealized experiments that restore euphotic-zone nutrients to zero (e.g., Sarmiento and Orr, 1991; Gnanadesikan et al., 2003) and more detailed experiments with an explicit representation of iron (e.g., Aumont et al., 2006; Jin et al., 2008). In particular, surface nutrients are not fully depleted under enhanced maximum phytoplankton growth rates in the Southern Ocean, because of light limitation in winter, under sea ice and in areas of deep mixed layers. This is illustrated in Fig. 5 by the surface phosphate fields simulated for model run COUPLED after switching to the enhanced phytoplankton maximum growth rate. Apart from a sensitivity experiment discussed below, the maximum growth rate is enhanced at all depth levels, although light limitation suppresses any significant

BGD

6, 4493–4525, 2009

CO₂ backflux matters

A. Oschlies

Title Page

Abstract

Introduction

Conclusions

References

Tables

Figures

◀

▶

◀

▶

Back

Close

Full Screen / Esc

Printer-friendly Version

Interactive Discussion



impact below about 130 m. For the idealized global scenario, the four different configurations ATCO2const, VEGconst, CONSTclim, and COUPLED are integrated over a period of 1000 years, for the regional scenarios the integration is limited to 100 years.

4.1 Temporal evolution

5 On switching to higher maximum growth rates, all model configurations show an initial peak in export production caused by a rapid consumption of surface nutrients left unutilized at the end of the model spin up. This peak in export production reaches 34 PgC/yr in the first year, i.e., about 27 PgC/yr above the normal level simulated by the control run with unchanged phytoplankton maximum growth rate. After 10 years, 10 the excess export production is already reduced to 9 PgC/yr, and it reaches 4 PgC/yr after 100 years and about 1.5 PgC/yr after 1000 years (Table 2, Fig. 6a). The enhanced maximum growth rates increase export production by more than 20% even after 1000 years of operation. However, apart from experiment ATCO2const, oceanic carbon uptake has saturated during this time and residual air-sea carbon fluxes are less than 15 0.03 PgC/yr in year 1000 (Fig. 6b). Accordingly, the oceanic uptake efficiency, which is defined here as the cumulative CO₂ air-sea flux to the cumulative excess export production, decreases with time and will eventually approach zero (Fig. 6c). The oceanic uptake efficiency is identical to the atmospheric uptake efficiency defined by Jin et al. (2008). The change in terminology reflects the fact that in experiments with interactive 20 terrestrial biosphere considered here (but not by Jin et al. (2008)), part of the carbon exchanged across the sea surface comes from the land. At the end of the 1000-year simulations with enhanced phytoplankton maximum growth rate, the ocean has taken up 190 PgC in run VEGconst, 460 PgC in run CLIMconst, 422 PgC in run COUPLED, and 1023 PgC in run ATCO2const (Table 3).

25 Qualitatively, the results of these millennial runs are very similar to those obtained in the previous section by varying the C:N ratio on centennial timescales: Experiment ATCO2const simulates the highest oceanic CO₂ uptake and VEGconst simulates the smallest oceanic carbon uptake (Fig. 7). The uptake simulated by the COUPLED and

Title Page

Abstract

Introduction

Conclusions

References

Tables

Figures

◀

▶

◀

▶

Back

Close

Full Screen / Esc

Printer-friendly Version

Interactive Discussion



CO₂ backflux mattersA. Oschlies

[Title Page](#)[Abstract](#)[Introduction](#)[Conclusions](#)[References](#)[Tables](#)[Figures](#)[Back](#)[Close](#)[Full Screen / Esc](#)[Printer-friendly Version](#)[Interactive Discussion](#)

CLIMconst runs is less than half of the uptake simulated by ATCO₂const. At the same time, it is more than twice as high as in run VEGconst. While the terrestrial carbon pool remains unchanged in runs ATCO₂const and VEGconst, it substantially decreases in CLIMconst and COUPLED (by 324 PgC and 263 PgC, respectively). That is, after 1000 years most of the additional carbon taken up by the ocean comes from the land and not from the atmosphere!

The relatively small difference in terrestrial carbon loss between experiments CLIMconst and COUPLED is due to the lower surface temperatures in the COUPLED experiment (Fig. 7d), which reduce the respiratory losses of carbon from the terrestrial carbon pool. Interestingly, experiment CLIMconst shows a decline of surface air temperatures by about 0.2°C within 1000 years although atmospheric CO₂ is assumed constant in the atmospheric radiation budget. This slight cooling is caused by changes in the albedo resulting from changes in terrestrial vegetation. In run CLIMconst, the lower atmospheric CO₂ leads to a shift from boreal forest with an albedo of 0.17 to tundra with an albedo of 0.22 over large parts of Asia and smaller parts of North America between about 60° N and 68° N.

Similar to the results of the previous section, the efficiency of the enhanced export production to take up carbon from the atmosphere and store it in the ocean differs considerably among the different model configurations (Fig. 6c). In model year 1000, the oceanic uptake efficiency amounts to 0.39 in run ATCO₂const and to only 0.065 in run VEGconst. The ratios diagnosed from experiments CLIMconst and COUPLED are 0.17 and 0.15, respectively.

4.2 Regional perturbations

Consistent with the findings of earlier studies (e.g., Gnanadesikan et al., 2003; Aumont et al., 2006), enhancing phytoplankton maximum growth rates in the tropics has only little impact on atmospheric CO₂, with reductions in all experiments being less than 8 μatm over 100 years in all experiments (Fig. 8a, dashed lines). This is mirrored in the simulated export production that is, after an initial enhancement during the first

few years, only marginally (7%) larger than that simulated by the unperturbed control run (Fig. 8c). Oceanic carbon uptake amounts to some 20–30 PgC after 100 years (Fig. 8b), with an air-sea CO₂ flux of about 0.1 PgC yr (Fig. 8d). In contrast, enhancing phytoplankton growth in the Southern Ocean is much more effective in the model, resulting in a much larger decline of atmospheric CO₂ levels and a much larger increase in export production, air-sea CO₂ flux and oceanic carbon uptake (Fig. 8, dotted lines). Typically, the impact of enhanced phytoplankton maximum growth in the Southern Ocean amounts to about 80% of the impact obtained when phytoplankton growth increased globally.

The oceanic uptake efficiency is relatively insensitive to the chosen perturbation area. For the COUPLED experiment, the oceanic uptake efficiency after 100 years is 0.29 for the global perturbation, 0.31 for the tropical perturbation, and 0.32 for the Southern Ocean perturbation (Fig. 9). In a sensitivity experiment in which the phytoplankton maximum growth rate was increased only in the first grid level of the model ($\Delta z=50$ m), the oceanic uptake efficiency increased to 0.36 for the tropical perturbation and to 0.33 for the Southern Ocean perturbation. This increase is consistent with the findings of Jin et al. (2008) who showed that an enhancement of phytoplankton growth close to the sea surface resulted in a higher fraction of exported carbon being derived from the atmosphere than for an enhancement of growth over the entire euphotic zone.

In terms of relative changes, the impacts of feedbacks from the atmospheric and terrestrial carbon pools are very similar among the different regional perturbations: After 100 years, simulated oceanic carbon uptake is about 100% higher compared to the VEGconst experiment when atmospheric $p\text{CO}_2$ is prescribed at a fixed level, and is more than 30% higher when both atmospheric and terrestrial carbon feedbacks are accounted for in run COUPLED. Compared to these differences, the impact of the climate feedback is small and amounts to a few percent only.

[Title Page](#)[Abstract](#)[Introduction](#)[Conclusions](#)[References](#)[Tables](#)[Figures](#)[◀](#)[▶](#)[◀](#)[▶](#)[Back](#)[Close](#)[Full Screen / Esc](#)[Printer-friendly Version](#)[Interactive Discussion](#)

5 Conclusions

This study was motivated by the considerable differences in published model-derived estimates of the impact of enhanced biological production on oceanic carbon uptake. Ocean-only studies that assumed a constant atmospheric $p\text{CO}_2$ (e.g., Schneider et al., 2004; Moore et al., 2006; Jin et al., 2008) typically predicted an oceanic carbon uptake about twice as high as estimates from coupled ocean-atmosphere studies that allowed atmospheric CO_2 to vary in response to air-sea CO_2 fluxes (e.g., Bopp et al., 2003; Gnanadesikan et al., 2003; Oschlies et al., 2008). While those investigators that assumed constant atmospheric CO_2 and generally obtained a high oceanic uptake efficiency acknowledged that their estimates were likely overestimates because of the choice of the atmospheric boundary condition, the magnitude of this overestimate has not yet been established. A first quantitative estimate is given in an as yet unpublished study of Sarmiento et al. (Sarmiento, J. L., Slater, R. D., Dunne, J., and Gnanadesikan, A.: Small scale carbon mitigation by patch fertilization) already referred to by Jin et al. (2008). In addition to the feedbacks originating from a finite atmospheric carbon reservoir, the current study also examined possible feedbacks from the terrestrial carbon pool.

Prescribing atmospheric $p\text{CO}_2$ rather than using an interactive atmospheric carbon pool implicitly assumes an infinite size of the atmospheric carbon reservoir. Under this assumption, the oceanic uptake efficiency turns out to be overestimated by about 25% on decadal timescales and about 100% on centennial timescales. The addition of an interactive terrestrial carbon pool on the atmospheric side of the sea surface can, to some extent, buffer changes in atmospheric $p\text{CO}_2$. The magnitude of this “buffering” effect depends on the $p\text{CO}_2$ sensitivity of the terrestrial biosphere. There is conclusive evidence that elevated atmospheric CO_2 concentrations stimulate net accumulation of carbon in terrestrial ecosystems (Luo et al., 2006), but the exact amount is still debated (e.g., Sokolov et al., 2008). The terrestrial component of the UVic model used here has a sensitivity of land carbon storage to atmospheric $p\text{CO}_2$ of about $1.2 \text{ PgC}/\mu\text{atm}$, which

BGD

6, 4493–4525, 2009

CO₂ backflux matters

A. Oschlies

Title Page

Abstract

Introduction

Conclusions

References

Tables

Figures

◀

▶

◀

▶

Back

Close

Full Screen / Esc

Printer-friendly Version

Interactive Discussion



is comparable or lower to sensitivities of other commonly used carbon cycle models (Friedlingstein et al., 2006). However, recent attempts to include the coupling of carbon and nitrogen cycles in the terrestrial biosphere have reported lower efficiencies of about 0.5 PgC/ μ atm (Thornton et al., 2007; Sokolov et al., 2008).

5 The terrestrial biosphere's $p\text{CO}_2$ sensitivity effectively increases the actual atmospheric carbon pool of 2.05 PgC/ μ atm seen by the ocean on the atmospheric side of the sea surface by almost 60% according to the UVic model sensitivity. This figure would reduce to 25% for the recent terrestrial models with coupled nitrogen and carbon cycles. For the current model, the oceanic carbon uptake in response to an enhance-
10 ment of the biological pump increases by a few percent on decadal timescales, by about 50% on centennial timescales, and by more than 100% on millennial timescales compared to a simulation that neglects feedbacks from the terrestrial carbon pool (Table 4). This impact is much larger than the feedback effects from climate change which, in the biological-pump perturbations modeled here, reduce the simulated oceanic CO_2
15 uptake by a few percent only.

The results of the idealized model experiments have revealed a considerable impact of atmospheric and terrestrial carbon feedbacks on estimated oceanic carbon uptake in response to changes in the biological carbon pump. On decadal to centennial timescales, model-derived estimates of oceanic carbon uptake can vary by up to a
20 factor 2, depending on the treatment of the atmospheric and terrestrial carbon pools. This can explain a substantial part of the difference reported by different previous studies. The results reported here are also relevant for attempts to assess the impacts of either natural or purposeful ocean fertilization. Any local enhancement of the biological pump will generate remote carbon fluxes, making a quantitative assessment of the net impact on atmospheric CO_2 difficult. Moreover, oceanic carbon uptake is not identical
25 to atmospheric CO_2 drawdown because of terrestrial carbon feedbacks.

Given our current understanding of global carbon feedbacks, the quantitative details of the idealized model experiments presented remain uncertain, although the sign of atmospheric and terrestrial carbon feedbacks and their impacts on fertilization-induced

[Title Page](#)[Abstract](#)[Introduction](#)[Conclusions](#)[References](#)[Tables](#)[Figures](#)[Back](#)[Close](#)[Full Screen / Esc](#)[Printer-friendly Version](#)[Interactive Discussion](#)

marine carbon uptake are expected to be robust. The results indicate the difficulties and inherent uncertainties we are still facing when trying to assess the impact of natural or purposeful ocean fertilization on atmospheric CO₂.

Acknowledgements. I thank Jorge Sarmiento for kindly providing a copy of a manuscript in preparation and Michael Eby for support with the UVic model. This study was supported by the Deutsche Forschungsgemeinschaft.

References

- Aumont, O. and Bopp, L.: Globalizing results from ocean in situ iron fertilization experiments, *Global Biogeochem. Cy.*, 20, GB2017, doi:10.1029/2005GB002591, 2006. 4503, 4505
- Bopp, L., Kohfeld, K. E., LeQuéré, C., and Aumont, O.: Dust impact on marine biota and atmospheric CO₂ during glacial periods, *Paleoceanography*, 18, 1046, doi:10.1029/2002PA000810, 2003. 4496, 4497, 4507
- Cox, P. M., Betts, R. A., Jones, C. D., Spall, S. A., and Totterdell, I. J.: Acceleration of global warming due to carbon-cycle feedbacks in a coupled climate model, *Nature*, 408, 184–187, 2000. 4498
- Duce, R. A., LaRoche, J., Altieri, K., et al.: Impacts of atmospheric anthropogenic nitrogen on the open ocean, *Science*, 320(5878), 893–897, 2008. 4495
- Engel, A., Delille, B., Jacquet, S., Riebesell, U., Rochelle-Newall, E., Terbrüggen, A., and Zondervan, I.: TEP and DOC production by *Emiliania huxleyi* exposed to different CO₂ concentrations: A mesocosm experiment, *Aquat. Microb. Ecol.*, 34, 93–104, 2004. 4500
- Friedlingstein, P., et al.: Climate-carbon cycle feedback analysis: Results from the C4MIP model intercomparison, *J. Climate*, 19, 3337–3353, 2006. 4502, 4508
- Gnanadesikan, A., Sarmiento, J. L., and Slater, R. D.: Effects of patchy ocean fertilization on atmospheric carbon dioxide and biological production, *Global Biogeochem. Cy.*, 17, 1050, doi:10.1029/2002GB001940, 2003. 4496, 4497, 4503, 4505, 4507
- Houghton, J. T., Meira Filho, L. G., Griggs, D. J., and Maskell, K.: Stabilization of atmospheric greenhouse gases: Physical, biological and socioeconomic implications, Intergovernmental Panel on Climate Change, World Meteorological Organization, Geneva, Technical Paper III, 1997. 4500

BGD

6, 4493–4525, 2009

CO₂ backflux matters

A. Oschlies

Title Page

Abstract

Introduction

Conclusions

References

Tables

Figures

◀

▶

◀

▶

Back

Close

Full Screen / Esc

Printer-friendly Version

Interactive Discussion



- Jin, X., Gruber, N., Frenzel, H., Doney, S. C., and McWilliams, J. C.: The impact on atmospheric CO₂ of iron fertilization induced changes in the ocean's biological pump, *Biogeosciences*, 5, 385–406, 2008, <http://www.biogeosciences.net/5/385/2008/>. 4496, 4497, 4503, 4504, 4506, 4507
- 5 Lampitt, R. S., Achterberg, E. P., Anderson, T. R., Hughes, J. A., Iglesias-Rodriguez, M. D., Kelly-Gerrey, B. A., Lucas, M., Popova, E. E., Sanders, R., Shepherd, J. G., Smythe-Wright, D., and Yool, A.: Ocean fertilization: a potential means of geoengineering?, *Philos. T. Roy. Soc. A.*, 366(1882), 3919–3945, 2008. 4495
- Luo, Y., Hui, D., and Zhang, D.: Elevated CO₂ stimulates net accumulations of carbon and nitrogen in land ecosystems: a meta-analysis, *Ecology*, 87, 53–63, 2006. 4507
- 10 Moore, J. K., Doney, S. C., Lindsay, K., Mahowald, N., and Michaels, A. F.: Nitrogen fixation amplifies the ocean biogeochemical response to decadal timescale variations in mineral dust deposition, *Tellus B*, 58, 560–572, 2006. 4495, 4497, 4507
- Orr, J. C., Maier-Reimer, E., Mikolajewicz, U., Monfray, P., Sarmiento, J. L., Toggweiler, J. R., Taylor, N. K., Palmer, J., Gruber, N., Sabine, C. L., Le Quéré, C., Key, R. M., and Boutin, J.: Estimates of anthropogenic carbon uptake from four three-dimensional global ocean models, *Global Biogeochem. Cy.*, 15, 43–60, 2001. 4496
- 15 Oeschlies, A. and Kähler, P.: Biotic contribution to air-sea fluxes of CO₂ and O₂ and its relation to new production, export production, and net community production, *Global Biogeochem. Cy.*, 18, GB1015, doi:10.1029/2003GB002094, 2004. 4496
- Oeschlies, A., Schulz, K. G., Riebesell, U., and Schmittner, A.: Simulated 21st century's increase in oceanic suboxia by CO₂-enhanced biological carbon export, *Global Biogeochem. Cy.*, 22, GB4008, doi:10.1029/2007GB003147, 2008. 4495, 4497, 4500, 4507
- 20 Riebesell, U., Zondervan, I., Rost, B., Tortell, P. D., Zeebe, R. E., and Morel, F. M. M.: Reduced calcification of marine plankton in response to increased atmospheric CO₂, *Nature*, 407, 364–367, 2000. 4495
- Riebesell, U., Schulz, K., Bellerby, R. G. J., Fritsche, P., Meyerhöfer, M., Neill, C., Nondal, G., Oeschlies, A., Wohlers, J., and Zöllner, E.: Enhanced biological carbon consumption in a high CO₂ ocean, *Nature*, 450, 545–548, 2007. 4495, 4500
- 30 Sarmiento, J. L. and Orr, J. C.: Three dimensional simulations of the impact of Southern Ocean nutrient depletion on atmospheric CO₂ and ocean chemistry, *Limnol. Oceanogr.*, 36, 1928–1950, 1991. 4503

BGD

6, 4493–4525, 2009

CO₂ backflux mattersA. Oeschlies

[Title Page](#)[Abstract](#)[Introduction](#)[Conclusions](#)[References](#)[Tables](#)[Figures](#)[◀](#)[▶](#)[◀](#)[▶](#)[Back](#)[Close](#)[Full Screen / Esc](#)[Printer-friendly Version](#)[Interactive Discussion](#)

Sarmiento, J. L. and Le Quéré, C.: Oceanic carbon dioxide uptake in a model of century-scale global warming, *Science*, 274, 1346–1350, 1996. 4495

Schmittner, A., Oschlies, A., Giraud, X., and Eby, M.: A global model of the marine ecosystem for multi-millennial simulations, *Global Biogeochem. Cy.*, 19, GB3004, doi:10.1029/2004GB002283, 2005. 4498

Schmittner, A., Oschlies, A., Matthews, H. D., and Galbraith, E. D.: Future changes in climate, ocean circulation, ecosystems and biogeochemical cycling simulated for a business-as-usual CO₂ emission scenario until 4000AD, *Global Biogeochem. Cy.*, 22, GB1013, doi:10.1029/2007GB002953, 2008. 4498

Schneider, B., Engel, A., and Schlitzer, R.: Effects of depth- and CO₂-dependent C:N ratios of particulate organic matter (POM) on the marine carbon cycle, *Global Biogeochem. Cy.*, 18, GB2015, doi:10.1029/2003GB002184, 2004. 4495, 4497, 4500, 4507

Sokolov, A. P., Kicklighter, D. W., Melillo, J. M., Felzer, B. S., Schlosser, C. A., and Cronin, T. W.: Consequences of considering carbon-nitrogen interactions on the feedbacks between climate and the terrestrial carbon cycle, *J. Clim.*, 21, 3776–3796, 2008. 4502, 4507, 4508

Thornton, P. E., Lamarque, J.-F., Rosenbloom, N. A., and Mahowald, N. M.: Influence of carbon-nitrogen cycle coupling on land model response to CO₂ fertilization and climate variability, *Global Biogeochem. Cy.*, 21, GB4018, doi:10.1029/2006GB002868, 2007. 4508

Volk, T. and Hoffert, M. I.: Ocean carbon pumps – Analysis of relative strengths and efficiencies in ocean-driven atmospheric CO₂ changes, in: *The Carbon Cycle and Atmospheric CO₂: Natural Variations, Archean to Present*, edited by: Sundquist, E. and Broecker, W., AGU Geophysical Monograph, Washington DC, 32, 99–110, 1985. 4495

Weaver, A. J., Eby, M., Wiebe, E. C., et al.: The UVic earth system climate model: Model description, climatology, and applications to past, present and future climates, *Atmos. Ocean*, 39, 361–428, 2001. 4498

BGD

6, 4493–4525, 2009

CO₂ backflux matters

A. Oschlies

Title Page

Abstract

Introduction

Conclusions

References

Tables

Figures

◀

▶

◀

▶

Back

Close

Full Screen / Esc

Printer-friendly Version

Interactive Discussion



Table 1. Simulated carbon inventories and flux changes.

Property	ATCO2const	VEGconst	COUPLED	CLIMconst
$p\text{CO}_2$	280	270.3	273.8	274.3
ΔC_{atm}	0 ^a	−19.8	−12.7	−11.7
ΔC_{ocn}	40.6	20.1	28.9	30.8
ΔC_{ter}	0	0	−14.1	−17.2
ΔSAT	0	−0.068	−0.031	−0.0015
ΔEP	1.40	1.45	1.44	1.40
ΔASE	0.53	0.27	0.37	0.39
$\int \Delta\text{ASE} / \int \Delta\text{EP}$	0.38	0.20	0.26	0.28

Experiments for $p\text{CO}_2$ -sensitive C:N ratios prescribed according to Fig. 2a. All numbers are model results for year 2100. Units are μatm for $p\text{CO}_2$ and PgC for changes in atmospheric, marine and terrestrial carbon pools (ΔC_{atm} , ΔC_{ocn} and ΔC_{ter}), and degrees Celcius for the change in globally averaged surface air temperature, ΔSAT . Fluxes are in PgC yr^{-1} for changes in export production (ΔEP) and air-sea CO_2 flux (ΔASE) with respect to the constant stoichiometry case. The last line is the ratio of time integrals of air-sea carbon flux and export production, respectively, from AD 1765 to AD 2100.

^a Total carbon is not conserved in experiment ATCO2const.

[Title Page](#)
[Abstract](#)
[Introduction](#)
[Conclusions](#)
[References](#)
[Tables](#)
[Figures](#)
[Back](#)
[Close](#)
[Full Screen / Esc](#)
[Printer-friendly Version](#)
[Interactive Discussion](#)


Table 2. Simulated changes in carbon fluxes for globally enhanced phytoplankton maximum growth rate.

Property	Time (yr)	ATCO2const	VEGconst	COUPLED	CLIMconst
ΔEP (Pg C yr ⁻¹)	1	26.8	26.8	26.8	26.8
	10	8.7	8.9	8.9	8.7
	100	4.1	5.3	5.0	4.1
	1000	1.64	1.15	1.35	1.54
ΔASE (Pg C yr ⁻¹)	1	9.8	9.6	9.5	9.5
	10	4.0	2.6	3.0	3.1
	100	1.8	0.40	0.96	1.1
	1000	0.33	-0.029	-0.011	0.016
$\int \Delta ASE / \int \Delta EP$	1	0.37	0.36	0.35	0.35
	10	0.47	0.37	0.39	0.39
	100	0.44	0.20	0.29	0.32
	1000	0.39	0.067	0.15	0.17

Title Page

Abstract

Introduction

Conclusions

References

Tables

Figures



Back

Close

Full Screen / Esc

Printer-friendly Version

Interactive Discussion



Table 3. Simulated carbon inventory changes for globally enhanced phytoplankton maximum growth rate.

Property	Time (yr)	ATCO2const	VEGconst	COUPLED	CLIMconst
$p\text{CO}_2$ (μatm)	1	280	276.8	277.0	277.0
	10	280	260.0	264.5	265.6
	100	280	218.1	240.5	247.1
	1000	280	190.2	204.5	215.6
ΔC_{ocn} (PgC)	1	9.74	9.51	9.42	9.42
	10	53.9	43.3	45.0	45.2
	100	269	131.0	186.3	193.3
	1000	1023	190.3	422.4	460.1
ΔC_{ter} (PgC)	1	0	0	-0.30	-0.33
	10	0	0	-11.4	-13.9
	100	0	0	-101.0	-121.4
	1000	0	0	-262.8	-323.6

The change in oceanic carbon, ΔC_{ocn} includes dissolved inorganic carbon and organic particulate carbon (the model does not explicitly resolve dissolved organic carbon or particulate inorganic carbon). In year 1, increases in organic matter account for about 25% of ΔC_{ocn} .

Title Page

Abstract

Introduction

Conclusions

References

Tables

Figures

◀

▶

◀

▶

Back

Close

Full Screen / Esc

Printer-friendly Version

Interactive Discussion



Table 4. Sensitivity of oceanic uptake efficiencies to atmospheric and terrestrial carbon feedbacks.

Experiment	$\frac{\text{ATCO}_2\text{const}}{\text{VEGconst}}$	$\frac{\text{COUPLED}}{\text{VEGconst}}$	$\frac{\text{CLIMconst}}{\text{COUPLED}}$
varC:N	1.94	1.32	1.09
maxgr.1 yr	1.02	0.99	1.00
maxgr.10 tr	1.26	1.04	1.00
maxgr.100 yr	2.23	1.46	1.09
maxgr.1000 yr	5.86	2.20	1.16
maxgr.S.Ocean	2.15	1.43	1.08
maxgr.tropics	1.83	1.33	1.06

Ratios of oceanic uptake efficiencies computed for ATMCO₂const, VEGconst, and CLIMconst, respectively, with respect to COUPLED. The experiments use $p\text{CO}_2$ -sensitive C:N ratios (varC:N) and enhanced phytoplankton maximum growth rates applied globally (maxgr.1 yr to maxgr.1000 yr), and over the Southern Ocean (maxgr.S.Ocean) and over the tropics (maxgr.tropics). Values are given for year 2100 for experiment varC:N and for model year 100 for the other experiments unless indicated otherwise in the experiment name.

[Title Page](#)
[Abstract](#)
[Introduction](#)
[Conclusions](#)
[References](#)
[Tables](#)
[Figures](#)




[Back](#)
[Close](#)
[Full Screen / Esc](#)
[Printer-friendly Version](#)
[Interactive Discussion](#)

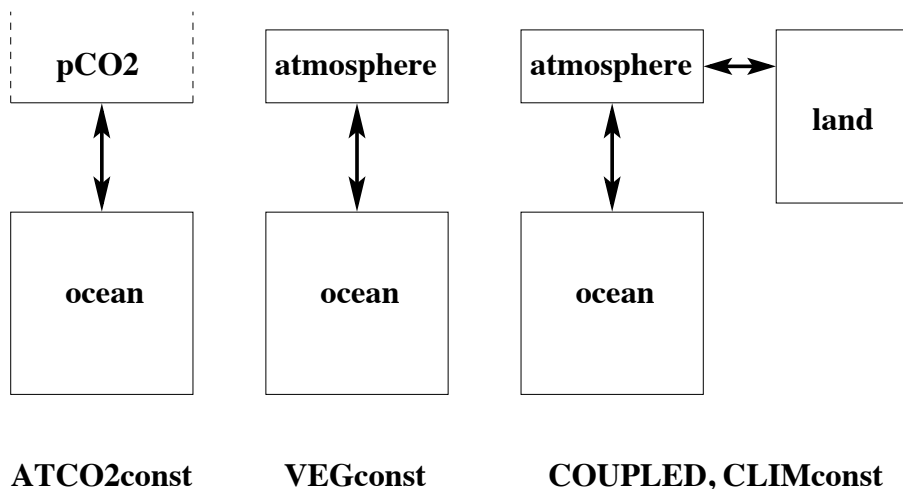



Fig. 1. Schematic design of the different model configurations used (see text). Shown are active carbon pools of configurations ATCO2const, VEGconst, COUPLED, and CLIMconst. Atmospheric $p\text{CO}_2$ is prescribed in ATCO2const, which corresponds to assuming an infinitely large atmospheric carbon reservoir. CLIMconst assumes constant $p\text{CO}_2$ in the atmospheric radiation budget and therefore simulates an essentially constant climate apart from possible CO₂ driven albedo changes.

[Title Page](#)
[Abstract](#)
[Introduction](#)
[Conclusions](#)
[References](#)
[Tables](#)
[Figures](#)
[◀](#)
[▶](#)
[◀](#)
[▶](#)
[Back](#)
[Close](#)
[Full Screen / Esc](#)
[Printer-friendly Version](#)
[Interactive Discussion](#)

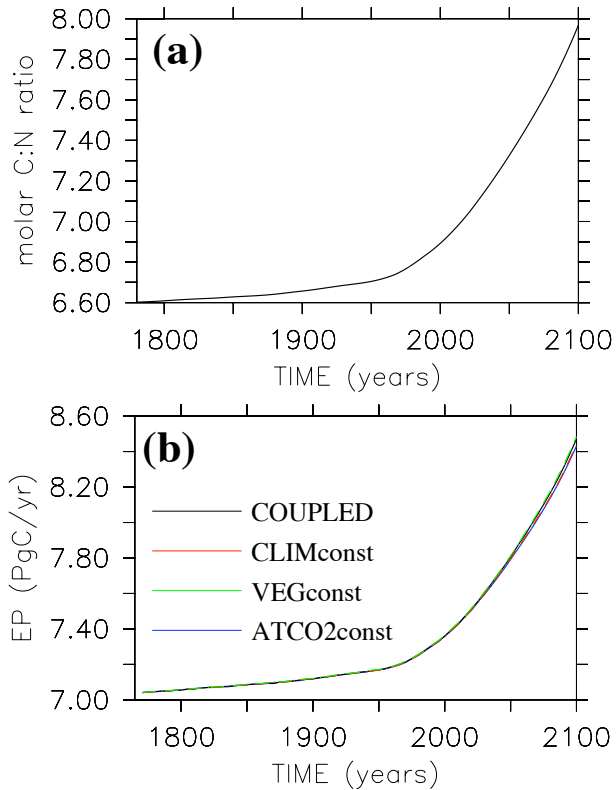



Fig. 2. (a) Time series of prescribed molar C:N ratio used in all experiments with varying C:N ratio. (b) Simulated export of organic carbon at $z=126$ m (in PgC/yr). Different colors refer to the different experiments (see text). The simulated export production is almost identical among the different model configurations.

Title Page

Abstract

Introduction

Conclusions

References

Tables

Figures



Back

Close

Full Screen / Esc

Printer-friendly Version

Interactive Discussion



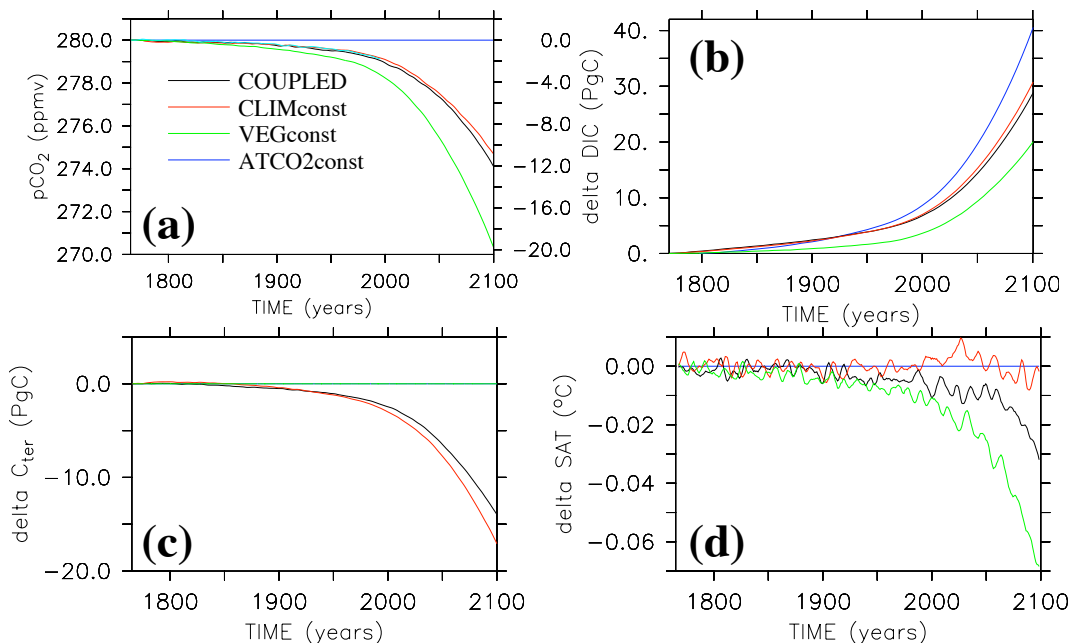


Fig. 3. Results of simulations with prescribed increase of C:N ratios (Fig. 2a): Simulated evolution of **(a)** atmospheric $p\text{CO}_2$ (in μatm), **(b)** oceanic carbon inventory referenced to initial state (in PgC), **(c)** terrestrial carbon (vegetation plus soils, in PgC), **(d)** global-mean surface air temperature (in °C), Solid black line refers to the fully coupled ocean-atmosphere-vegetation model, red line to a configuration with atmospheric CO_2 assumed as $280 \mu\text{atm}$ in the atmospheric radiation routine, green line to a configuration with constant terrestrial carbon pool, and the blue line to a configuration with prescribed atmospheric $\text{CO}_2 = 280 \mu\text{atm}$.

[Title Page](#)
[Abstract](#)
[Introduction](#)
[Conclusions](#)
[References](#)
[Tables](#)
[Figures](#)
[◀](#)
[▶](#)
[◀](#)
[▶](#)
[Back](#)
[Close](#)
[Full Screen / Esc](#)
[Printer-friendly Version](#)
[Interactive Discussion](#)

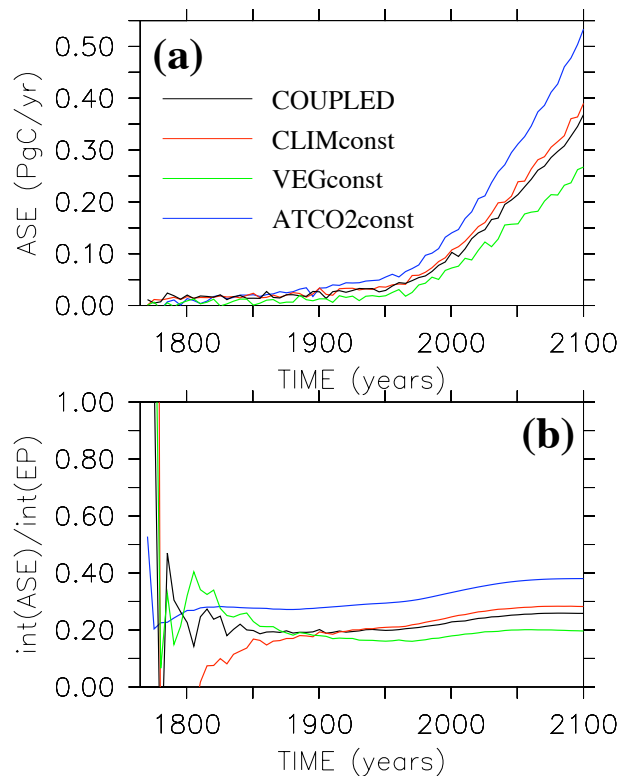



Fig. 4. Results of experiment with prescribed increase of C:N ratios (Fig. 2a): **(a)** Simulated air-sea gas exchange of CO₂ (in PgC/yr). **(b)** Ratio of cumulative air-sea carbon flux to simulated export of organic carbon across $z=126$ m. Color code as in previous figures.

[Title Page](#)[Abstract](#)[Introduction](#)[Conclusions](#)[References](#)[Tables](#)[Figures](#)[◀](#)[▶](#)[◀](#)[▶](#)[Back](#)[Close](#)[Full Screen / Esc](#)[Printer-friendly Version](#)[Interactive Discussion](#)

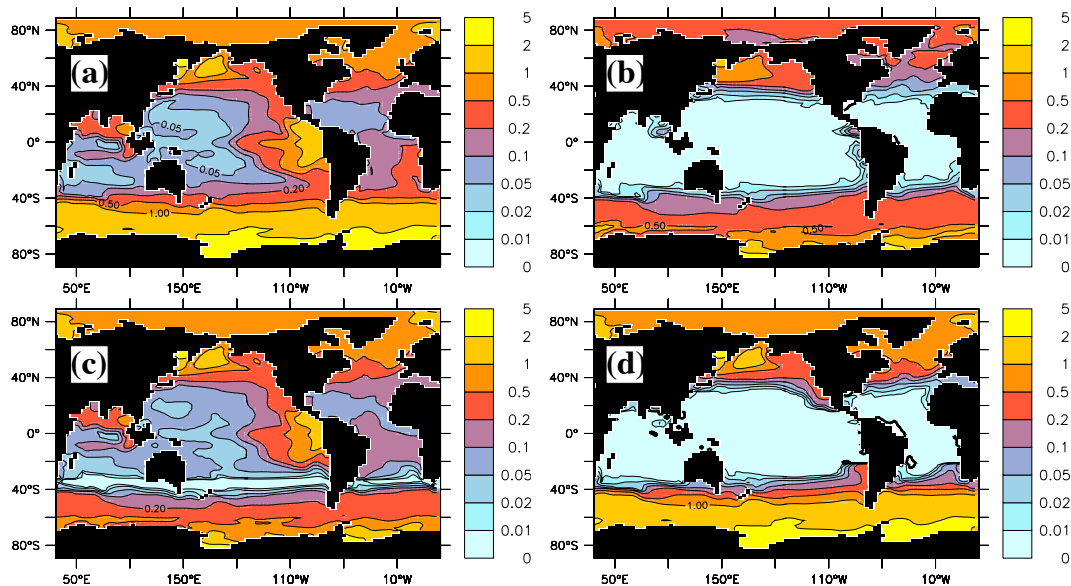


Fig. 5. Surface phosphate concentrations simulated by (a) the control experiment, (b) the experiment with globally enhanced phytoplankton maximum growth rates, (c) the experiments with maximum phytoplankton growth rates enhanced south of 30° S, and (d) with maximum phytoplankton growth rates enhanced in the tropical belt between 18° S and 18° N. All results are shown for model year 100, but look virtually identical already a few years after the onset of the perturbation. Units are $\text{mmol PO}_4 \text{ m}^{-3}$.

[Title Page](#)
[Abstract](#)
[Introduction](#)
[Conclusions](#)
[References](#)
[Tables](#)
[Figures](#)
[⏪](#)
[⏩](#)
[◀](#)
[▶](#)
[Back](#)
[Close](#)
[Full Screen / Esc](#)
[Printer-friendly Version](#)
[Interactive Discussion](#)

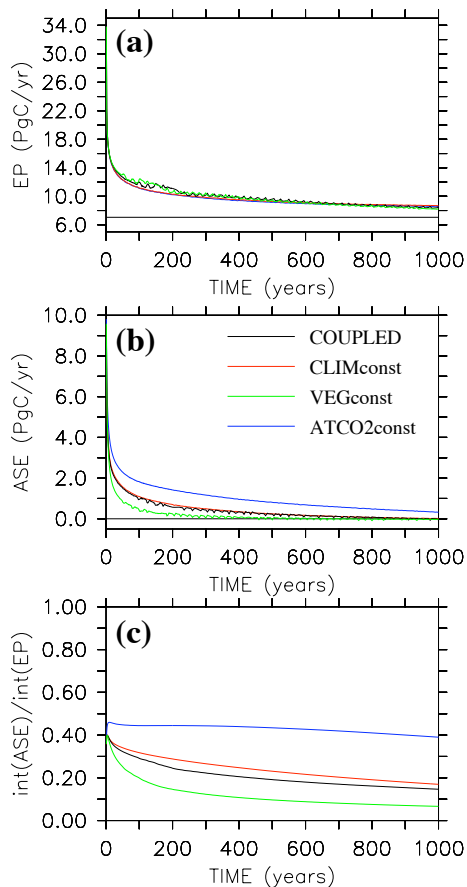



Fig. 6. Simulations with globally enhanced phytoplankton maximum growth rates: **(a)** Simulated export of organic carbon at $z=126$ m (in PgC/yr). **(b)** Simulated air-sea gas exchange of CO₂ (in PgC/yr). **(c)** Ratio of cumulative air-sea carbon flux to simulated export of organic carbon across $z=126$ m. Color code as in previous figures.

[Title Page](#)
[Abstract](#) [Introduction](#)
[Conclusions](#) [References](#)
[Tables](#) [Figures](#)
[◀](#) [▶](#)
[◀](#) [▶](#)
[Back](#) [Close](#)
[Full Screen / Esc](#)
[Printer-friendly Version](#)
[Interactive Discussion](#)



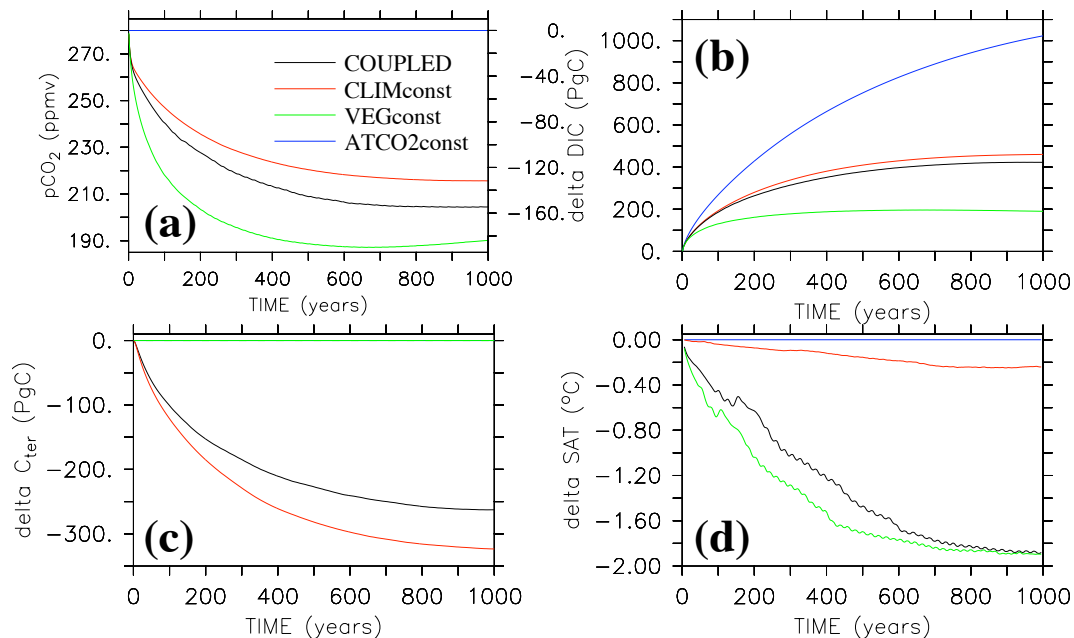


Fig. 7. Simulations with globally enhanced phytoplankton maximum growth rates: Simulated evolution of (a) atmospheric $p\text{CO}_2$ (in μatm), (b) oceanic carbon inventory referenced to initial state (in PgC), (c) terrestrial carbon (vegetation plus soils, in PgC), (d) global-mean surface air temperature (in degree Celsius). Color code as in previous figures.

Title Page

Abstract

Introduction

Conclusions

References

Tables

Figures

◀

▶

◀

▶

Back

Close

Full Screen / Esc

Printer-friendly Version

Interactive Discussion



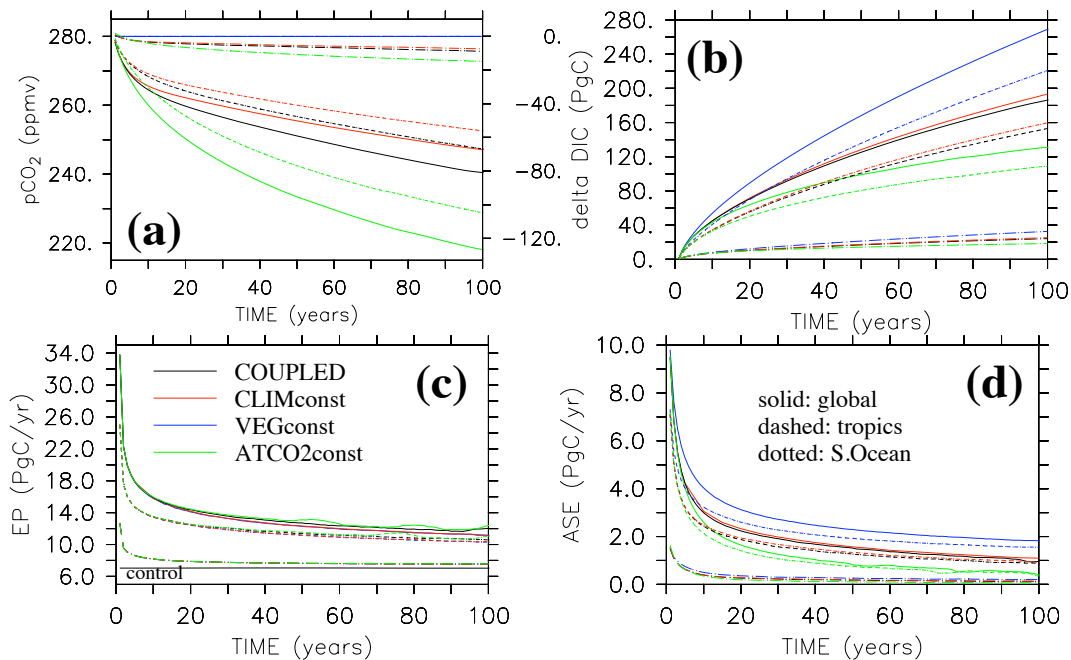


Fig. 8. Simulations with enhanced phytoplankton growth rates applied globally (solid lines), to the tropical ocean between 18° S and 18° N (dashed lines), and to the Southern Ocean south of 30° S (dotted lines). **(a)** Simulated atmospheric $p\text{CO}_2$ (in μatm , left axis, and in PgC, right axis), **(b)** oceanic carbon uptake (in PgC), **(c)** export production (in PgC/yr), and **(d)** air-sea CO₂ exchange (in PgC/yr). Color code as in previous figures.

Title Page

Abstract

Introduction

Conclusions

References

Tables

Figures

◀

▶

◀

▶

Back

Close

Full Screen / Esc

Printer-friendly Version

Interactive Discussion



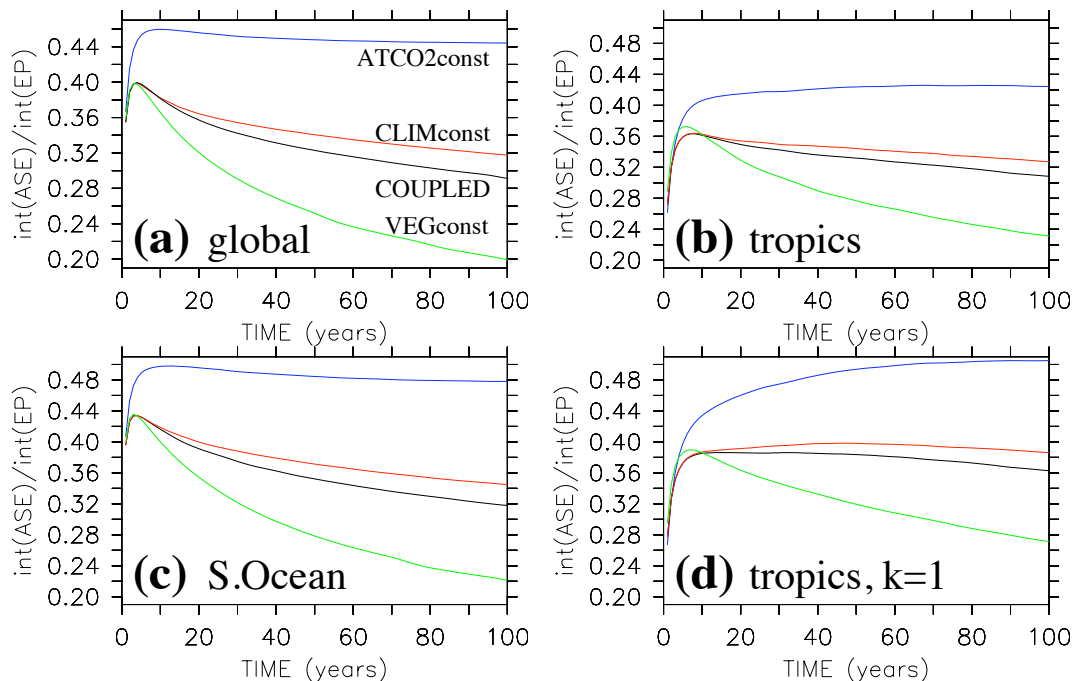


Fig. 9. Ratio of cumulative air-sea CO₂ flux to cumulative export production for experiments with enhanced phytoplankton maximum growth rates applied **(a)** globally, **(b)** to the tropics between 18° S and 18° N, **(c)** to the Southern Ocean south of 30° S, and **(d)** to the uppermost grid box in the tropics between 18° S and 18° N. Color code as in previous figures.

[Title Page](#)
[Abstract](#)
[Introduction](#)
[Conclusions](#)
[References](#)
[Tables](#)
[Figures](#)
[◀](#)
[▶](#)
[◀](#)
[▶](#)
[Back](#)
[Close](#)
[Full Screen / Esc](#)
[Printer-friendly Version](#)
[Interactive Discussion](#)

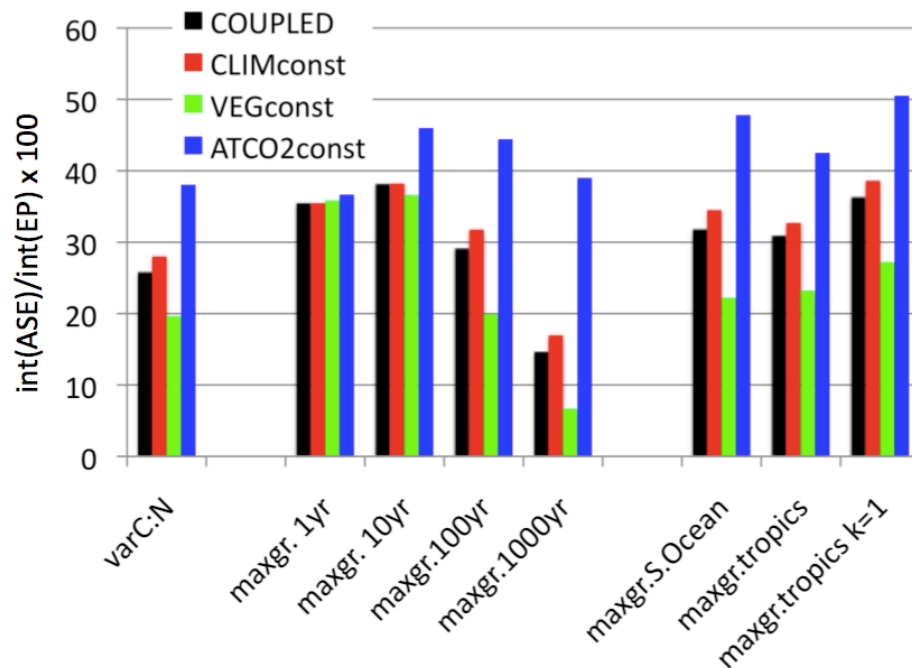



Fig. 10. Compilation of the oceanic uptake efficiency, i.e., the ratio of cumulative air-sea CO₂ flux to cumulative export production for the different experiments. “varC:N” refers to the experiments with prescribed increase of C:N ratios (Sect. 3), “maxgr.” refers to the experiments with enhanced phytoplankton maximum growth rate (Sect. 4). For each experiment, different colors refer to the different model configurations.

[Title Page](#)
[Abstract](#)
[Introduction](#)
[Conclusions](#)
[References](#)
[Tables](#)
[Figures](#)
[I◀](#)
[▶I](#)
[◀](#)
[▶](#)
[Back](#)
[Close](#)
[Full Screen / Esc](#)
[Printer-friendly Version](#)
[Interactive Discussion](#)
